



J. Serb. Chem. Soc. 78 (12) 2017–2037 (2013)
JSCS–4548

Journal of
the Serbian
Chemical Society

JSCS-info@shd.org.rs • www.shd.org.rs/JSCS

UDC 546.98+667.287:539.24:66.094.1

Original scientific paper

Electrochemical and nanogravimetric studies of palladium phthalocyanine microcrystals*

ÁKOS NEMES, COLIN E. MOORE and GYÖRGY INZELT*

*Department of Physical Chemistry, Institute of Chemistry, Eötvös Loránd University,
Pázmány Péter sétány 1/A, 1117 Budapest, Hungary*

(Received 9 September, revised 19 September 2013)

Abstract: An electrochemical quartz crystal nanobalance was used to study the redox behavior of palladium phthalocyanine microcrystals attached to gold and platinum in aqueous solutions at different pH values. In order to investigate the substrate effect, paraffin impregnated graphite electrodes were also applied. It was found that the redox transformations of palladium phthalocyanine are accompanied with deprotonation–protonation as well as the sorption and desorption of counter-ions, the extent of which depend on the pH. Based on the results of the nanogravimetric measurements, a redox mechanism describing the pH dependence is suggested. Simultaneously with charge transfer processes, solid–solid phase transitions and water transport occur.

Keywords: palladium phthalocyanine; microcrystals; electrochemical quartz crystal nanobalance (EQCN); redox transformations; solid–solid phase transition.

INTRODUCTION

The first phthalocyanine (iron phthalocyanine) was discovered by chance in 1928 during the industrial production of phthalimide, and it was first studied in detail by Linstead. Linstead published a series of papers devoted to the preparation and characterization of several phthalocyanines, and he also proposed the structure of this class of compounds.¹ Investigations of the electrochemical behavior of phthalocyanines have been in the foreground of research during the last 30 years,^{2–46} (and citations therein) especially as a catalyst of the oxygen reduction reaction, since it is of utmost importance to find a suitable and cheap catalyst that could replace the expensive platinum. A wide range of other applications

*Corresponding author. E-mail: inzeltgy@chem.elte.hu

doi: 10.2298/JSC130909094N

• This paper is dedicated to Professor Branislav Nikolić on the occasion of his 70th birthday with the acknowledgement of his outstanding contributions to the development of electrochemistry.

2017



beside catalysis, such as in electrochromic display devices, in electrochemical power sources including solar cells and in sensors has been put forward. However, elucidation of the electrochemical processes occurring during the redox transformations of phthalocyanines is an interesting and challenging task in itself. A survey of the literature revealed that there are not two similar cyclic voltammograms on a given phthalocyanine in papers devoted to the study of this group of compounds. The main reason is that the voltammetric and other (*e.g.*, spectroscopic) responses of the phthalocyanine ring (Pc) strongly depend on metal ions in the centre of the ring, the substituents on the periphery of the macrocyclic ring, the solvent and the electrolyte used (especially when complex forming agents are present), the presence of oxygen, temperature and even the morphology of the surface layer (adsorbed or deposited by different methods). A further difficulty in the comparison of the results is that in the majority of the cases, substituted phthalocyanines were used to make the compound soluble. Many diverse processes, including irreversible ones, can occur, such as the formation of peroxy and oxo-bridged species in contact with oxygen in solution or even in solid form, or nucleation-growth-like phase transition in the solid layer during redox processes. The variety of the shapes of the voltammograms is due to thermodynamic reasons and to kinetic effects.

According to theoretical considerations, if the *d* orbitals of a metal are positioned between HOMO and LUMO gap of the phthalocyanine (Pc^{2-}) ligand, *e.g.*, this is the case for Co and Fe, the redox transformation of the central metal ion can be observed, especially if suitable coordinating species are present in the solution. For other metal phthalocyanines, such as Cu, Ni, Zn, Pt and Pd, the metal ions do not participate in redox processes, only the Pc ring will be oxidized or reduced.^{14,15,29,30} A wide arsenal of non-electrochemical methods have been used to characterize the different phthalocyanines, however, the electrochemical quartz crystal nanobalance (EQCN) has not yet been exploited, only platinum phthalocyanine microcrystals in contact with aqueous sulfuric acid and sodium sulfate solutions³³ and palladium phthalocyanine films in non-aqueous solutions²⁹ have been studied by this technique. While FePc, CoPc, MnPc, MgPc, *etc.*, have been thoroughly investigated, only few of studies have been devoted to PtPc^{19–23,28,33} and PdPc.^{29–31}

In the present study, our attention was focused on an EQCN study of palladium phthalocyanine (PdPc) microcrystals attached to different substrates and investigated under different conditions.

EXPERIMENTAL

Palladium phthalocyanine (PdPc) (Merck) was used without further purification. Analytical grade chemicals such as H_2SO_4 (Merck), Na_2SO_4 (Merck) and NaOH (Sigma–Aldrich) were used as received. Doubly distilled water was used (Millipore water). A sodium chloride saturated calomel electrode (SCE) was used as the reference electrode, which was carefully

separated from the main compartment by a double frit. A platinum or a gold wire served as the counter electrode. Cycling of the potential as a pretreatment of the electrode was performed before each experiment in the supporting electrolyte, until a voltammogram characteristic of a clean Au, Pt or PIGE electrode was obtained. Phthalocyanine microcrystals were attached to the gold, platinum or paraffin impregnated graphite (PIGE) surface (surface area, $A = 0.196 \text{ cm}^2$) either by mechanical abrasion or from a sonicated phthalocyanine–2-propanol sol *via* dropping an adequate amount of the suspension and drying it. The sonification was realized using a Realsonic 57, Korea.

Five-MHz AT-cut crystals of 2.54 cm diameter coated with gold or platinum (Stanford Research Systems, SRS, U.S.A.) were used in the EQCN measurements. The electrochemically and the piezoelectrically active areas were 1.37 and 0.4 cm^2 , respectively. The integral sensitivity of the crystals (C_p) was found to be $56.6 \times 10^6 \text{ Hz g}^{-1} \text{ cm}^2$, *i.e.*, 1 Hz corresponded to 17.7 ng cm^{-2} . The integral sensitivity was calculated from the frequency change measured during silver deposition / dissolution or from the electroreduction of gold oxide using the “effective” charge related to the piezoelectrically active area, *i.e.*, the total charge consumed during the calibration was multiplied by the ratio of the piezoelectrically active and the electrochemically active areas. The experimental setup and conditions were the same as those previously reported.^{47,48} The apparent molar mass of the deposited or the exchanged species (M) was calculated from the slope of the Δf vs. Q curve using the following formula: $M = (nFA/C_p) d\Delta f/dQ$, where n is the number of electrons involved in the electrochemical reaction, F is the Faraday constant, Δf is the frequency change, Q is the charge consumed and A is the electrode surface area. Although the requirements (uniform and homogeneous surface layer) for the application of the Sauerbrey Equation⁴⁹ were not strictly met, based on the measured frequency values, a rough estimation could be performed. The relative values of Δf obtained for the incorporation of different ions and solvent molecules, however, should be approximately correct. The crystals were mounted in a holder made from Kynar® (poly(vinylidene fluoride)) and connected to a SRS QCM 200 unit. Either an Elektroflex 453 potentiostat or a Biologic VSP potentiostat and a Universal Frequency Counter PM6685 (Fluke) connected to an IBM personal computer were used for the control of the measurements and for data acquisition.

Simultaneously with the frequency, the surface resistance (loss) was also monitored. As it remained constant, the behavior of the surface layer consisting of microcrystals remained elastic during the electrochemical transformations, *i.e.*, no viscoelastic effect appeared.

RESULTS AND DISCUSSION

Cyclic voltammetric and EQCN responses for freshly prepared layers

Figure 1 shows a series of consecutive cyclic voltammograms obtained for PdPc microcrystals deposited on PIGE in contact with deaerated sulfuric acid solution. During cycling, four anodic waves and three cathodic waves developed; waves II_a , II_c and IV_c continuously increased, as can be seen in Fig. 1. However, this pattern depended on several factors: potential limits, presence or absence of oxygen, the type of the substrate, the nature and concentration of the electrolyte, the layer thickness and the deposition method.

This type of voltammogram developed only if the positive potential limit was higher than 1 V vs. SCE, *i.e.*, if the region of the oxidation at peak I_a was achieved in acidic solutions. For the re-reduction of the PdPc, relatively high

negative potential, higher than *ca.* -0.35 V had to be applied. The irreversible nature of the voltammetric wave indicates that a chemical reaction was coupled to electron transfer steps. The big difference between the anodic and cathodic peaks could be related to a phase transition in the solid layer of microcrystals. The peaks were named in series according to the order of their potential. Peak IV_c obviously belonged to the anodic waves I_a and II_a , since the charge injected (electrons removed) was regained in the potential region of IV_c .

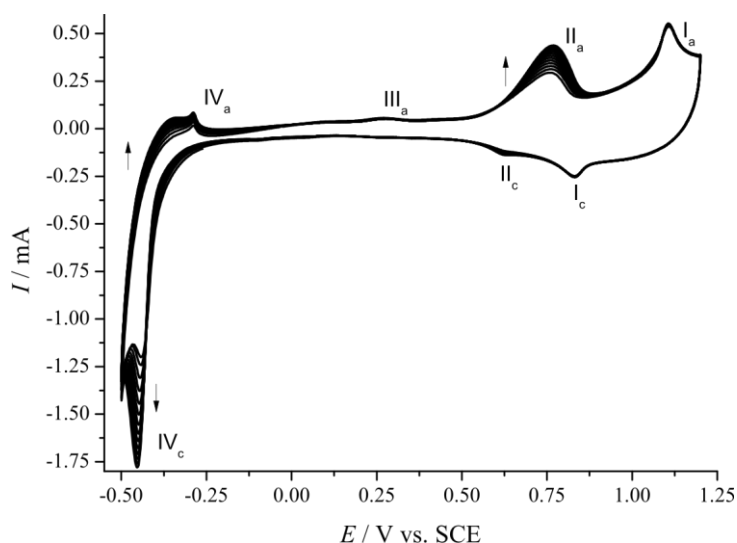


Fig. 1. Consecutive cyclic voltammograms (14 cycles) obtained for PdPc microcrystals deposited on PIGE. Electrolyte: 1 mol dm^{-3} deaerated sulfuric acid. Scan rate: 100 mV s^{-1} .

The very first cycle always differs from the subsequent ones, as can be seen in Fig. 2. Figure 2 also shows the effect of the positive potential limit since during the first cycle when the switching potential was set to 1 V, only a small current increase commenced at *ca.* 0.8 V but when 1.4 V was chosen as the positive potential limit, peak I_a became a well-developed peak and the I_c wave also appeared. The third cycle was started from -0.5 V, and while the reduction currents remained practically the same, three oxidation waves (I_a , II_a , III_a and IV_a) could be seen; peak I_a became smaller and shifted in the direction of less positive potentials.

The EQCN results revealed that a mass increase occurred simultaneously with the charge injection, which could be related to the incorporation of counter ions and water molecules in the layer of microcrystals (Fig. 3). The average molar mass derived for the interval between 0.9 and 1 V was $M = 126 \pm 15 \text{ g mol}^{-1}$, which somewhat increased in the course of consecutive cycles. However, at the beginning of the oxidation, a much smaller value, $M = 28 \pm 3 \text{ g mol}^{-1}$ was

obtained, while close to the 1 V limit, this value increased to $M = 259 \pm 25 \text{ g mol}^{-1}$, which indicated that the very first process was deprotonation, and the anions entered the layer in a later phase of the oxidation.

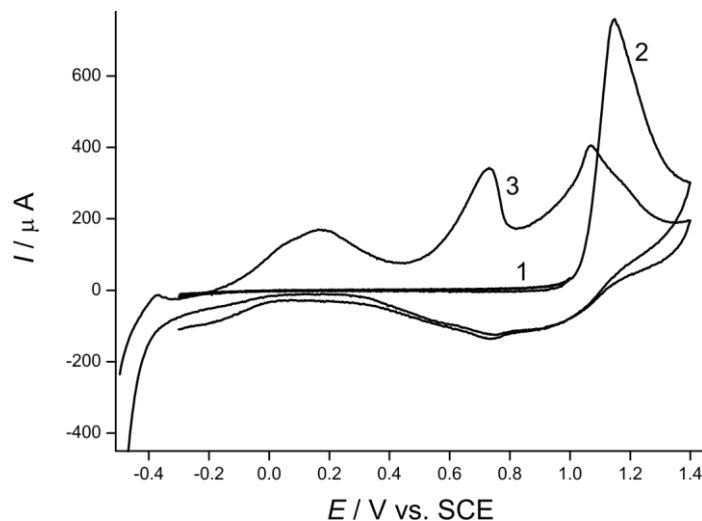


Fig. 2. Cyclic voltammograms obtained for a freshly prepared PdPc layer of microcrystals deposited on PIGE. Electrolyte: 0.5 mol dm^{-3} non-deaerated sulfuric acid. Scan rate: 100 mV s^{-1} . Potential limits were as follows: 1) first cycle from -0.3 to 1 V , 2) second cycle from -0.3 to 1.4 V and 3) third cycle from -0.5 to 1.4 V .

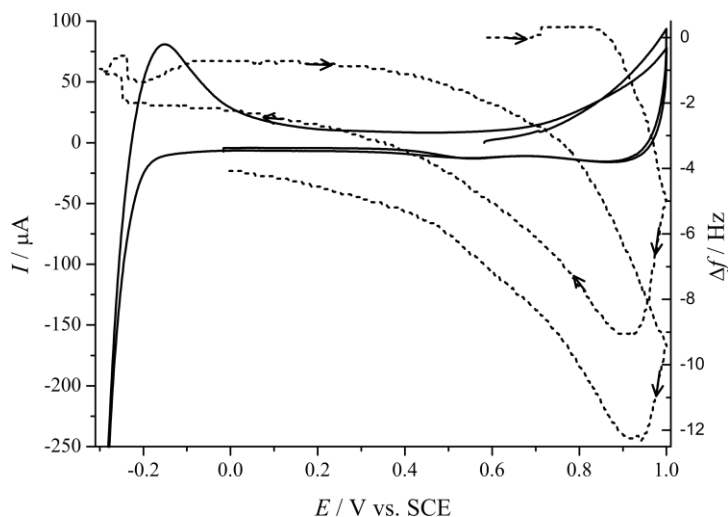


Fig. 3. Cyclic voltammograms (solid line) and the simultaneously obtained EQCN frequency changes (dotted line) for a freshly deposited PdPc layer of microcrystals on Au. Cycling was started from the open-circuit potential. Electrolyte: 1 mol dm^{-3} deaerated sulfuric acid. Scan rate: 20 mV s^{-1} .

However, this effect was observed only during the conditioning period. If the positive potential limit was set above 1 V, a mass decrease was observed, which was due to the dissolution of the microcrystals (Fig. 4). This dissolution or delamination of a portion of PdPc ceased after several cycles and both the cyclic voltammogram and the EQCN curve remained stable thereafter, providing that the experimental conditions, *e.g.*, the potential limit of cycling, remained the same.

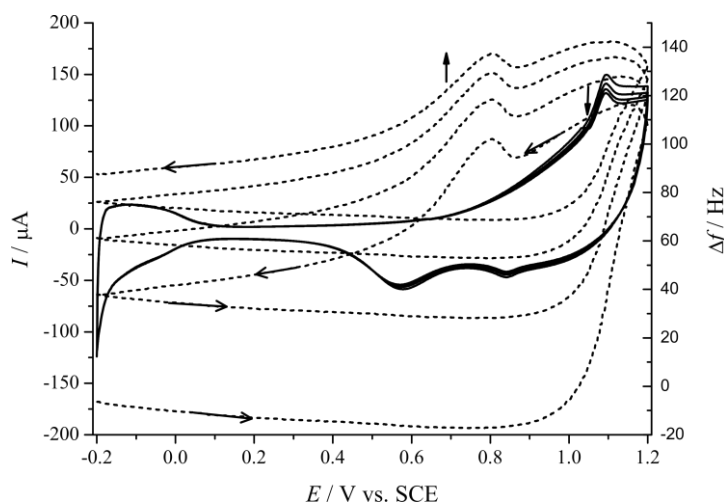


Fig. 4. Consecutive cyclic voltammograms (solid line) and the simultaneously obtained EQCN frequency changes (dotted line) for PdPc microcrystals on Au. Electrolyte: 1 mol dm⁻³ deaerated sulfuric acid. Scan rate: 20 mV s⁻¹.

Effect of the positive potential limit

The importance of the potential limits has already been emphasized. However, a closer look at this effect revealed an interesting phenomenon. While – as expected – the development of peak I_a and the respective peak I_c occurred gradually if the potential exceeds *ca.* 1 V, wave II_c appeared even when the positive potential did not reach this region. The EQCN frequency changes, however, evidenced that a different process started at lower potentials. Below *ca.* 1 V, a frequency increase occurred, while above it, a frequency decrease started. It follows that in the first phase of oxidation, the oxidation was accompanied by deprotonation, and anions entered the layer only at higher positive potentials. The latter process continued even during the cathodic half-cycle (Fig. 5).

Effect of the presence of oxygen

As seen in Fig. 6, in the presence oxygen the pair of waves II_a and II_c does not appear, I_a and I_c increase, and oxygen reduction starts at *ca.* 0.1 V. However, it is true only of layers after many cycles. (Voltammograms displayed on Figs. 1 and 6 were obtained for the same layer of microcrystals.) For a virgin layer, even

in the presence of oxygen, wave II_a appears and wave III_a, which is usually only a very small one, presents itself as a well-developed peak (Fig. 2).

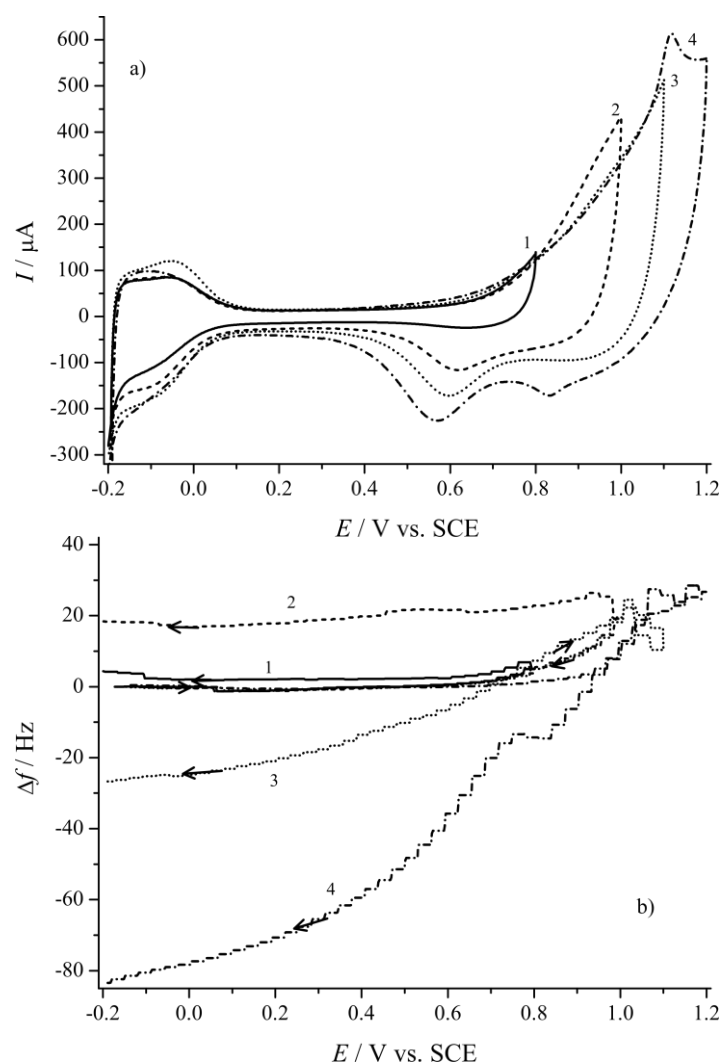


Fig. 5. a) Cyclic voltammograms and b) the simultaneously obtained EQCN frequency changes for PdPc microcrystals on Pt at different positive potential limits. Electrolyte: 1 mol dm^{-3} deaerated sulfuric acid. Scan rate: 20 mV s^{-1} .

In the case of PtPc, it is claimed that peak II_a is associated with the oxidation of the phthalocyanine at, or near to the $\text{Au} | \text{PtPc}$ interface, and develops during repetitive cycling.^{23,33} However, this statement is somewhat contradictory since it is to be expected that this wave would appear at the early phase of oxidation and would increase continuously. However, as it does not develop in the presence

of oxygen when PIGE and Au were substrates or when a Pt electrode was used, it could be concluded that it is rather due to the absence of interaction with oxygen. In the case of the Pt substrate, it could be explained by the interaction with PtO, which already appears in this potential range. Therefore, it is more likely that peak II_a does not appear if oxo or peroxy-bridged compounds are present (peroxy species are formed at low potentials).

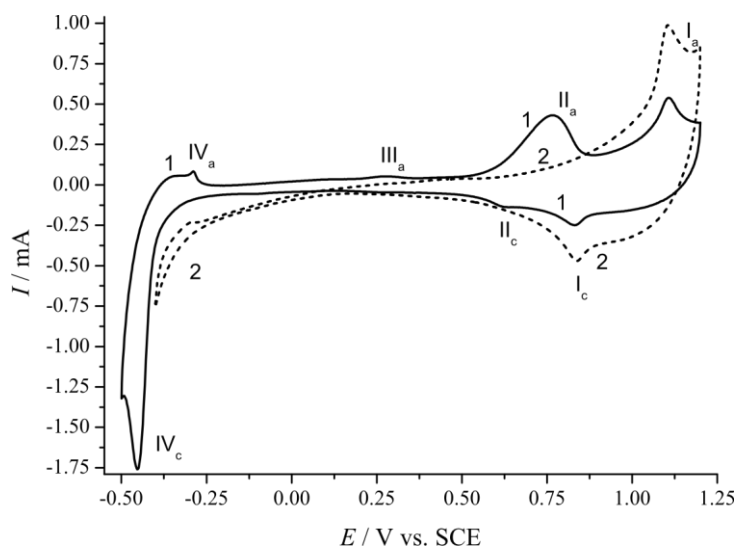


Fig. 6. Cyclic voltammograms obtained for PdPc microcrystals deposited on PIGE. Electrolyte: 1) 1 mol dm⁻³ deaerated and 2) oxygen saturated sulfuric acid. Scan rate: 100 mV s⁻¹.

Effect of scan rate

The scan rate dependence for a PIGE–PdPc system under an argon atmosphere is shown in Fig. 7. From the current (*I*) vs. scan rate (*v*) plots, it could be concluded that both I_a–I_c and II_a–II_c are surface waves since the function is linear, and the peak potential does not shift substantially with scan rate. In the potential region of wave IV_c, hydrogen evolution overlaps with the reduction of PdPc, which renders such analysis meaningless.

However, in the case of thick layers of microcrystals at higher scan rates, the cyclic voltammetric response becomes diffusional (Fig. 8).

It is even more noteworthy that at higher scan rates, the incorporation of the ionic species and especially of water, which is probably the slowest process, are incomplete. The shape of the cyclic voltammograms remain practically unaltered, *i.e.*, the relative slowness of the anion incorporation is responsible for the diffusional behavior at high scan rates, while the lag of the water sorption is responsible for the incomplete mass change during the positive-going scan.

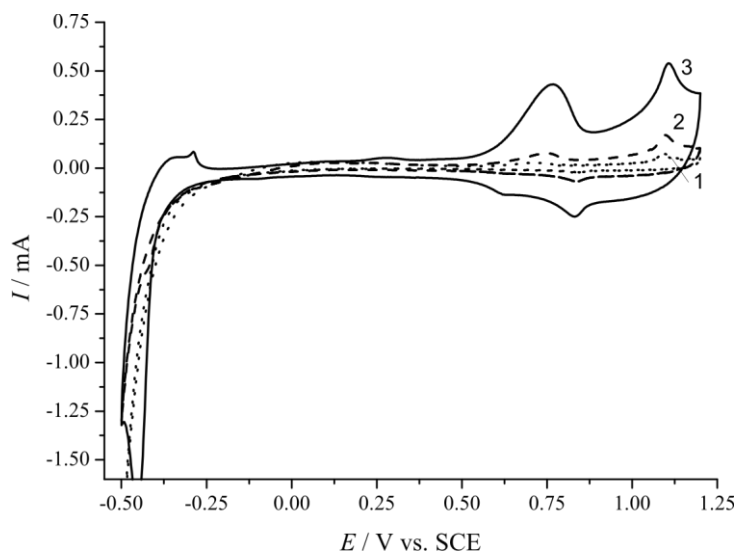


Fig. 7. Cyclic voltammograms obtained for PdPc microcrystals deposited on PIGE. Electrolyte: 1 mol dm⁻³ deaerated sulfuric acid. Scan rates: 1) 5, 2) 20 and 3) 100 mV s⁻¹.

Base line corrections

In the case of PIGE and gold, very low anodic current flows in the potential region of interest, and the oxide-reduction current, which might be substantial, is also small if the positive potential limit applied is less than 1.25 V. On the other hand, for platinum in both the hydrogen underpotential deposition (H-UPD) region and the oxide region substantial anodic and cathodic currents, respectively, arise. In the case of the calculation of the apparent molar mass value for the exchanged species, the charge and the frequency change should be corrected. The comparison when a gold substrate was used is shown in Fig. 9.

The cyclic voltammogram of PdPc shown in Fig. 9a does not show any contribution from the reduction of gold oxide. Furthermore, the EQCN frequency response (Fig. 9b) obtained for Au-PdPc was orders of magnitude higher than that of the gold electrode, *i.e.*, the surface of the gold electrode was covered by PdPc and the contribution from the gold substrate was negligible. It was also observed that even at high positive potential limits, the formation of gold oxide was hindered in the presence of PdPc.

As seen in Fig 10, in the case of platinum, the background current should be taken into account, even though both hydrogen adsorption in the H-UPD region and oxide formation are somewhat hindered by the surface PdPc layer of microcrystals. On the other hand, the EQCN response originating from the platinum oxide formation and reduction are negligibly small compared with the frequency change due to the PdPc crystals.

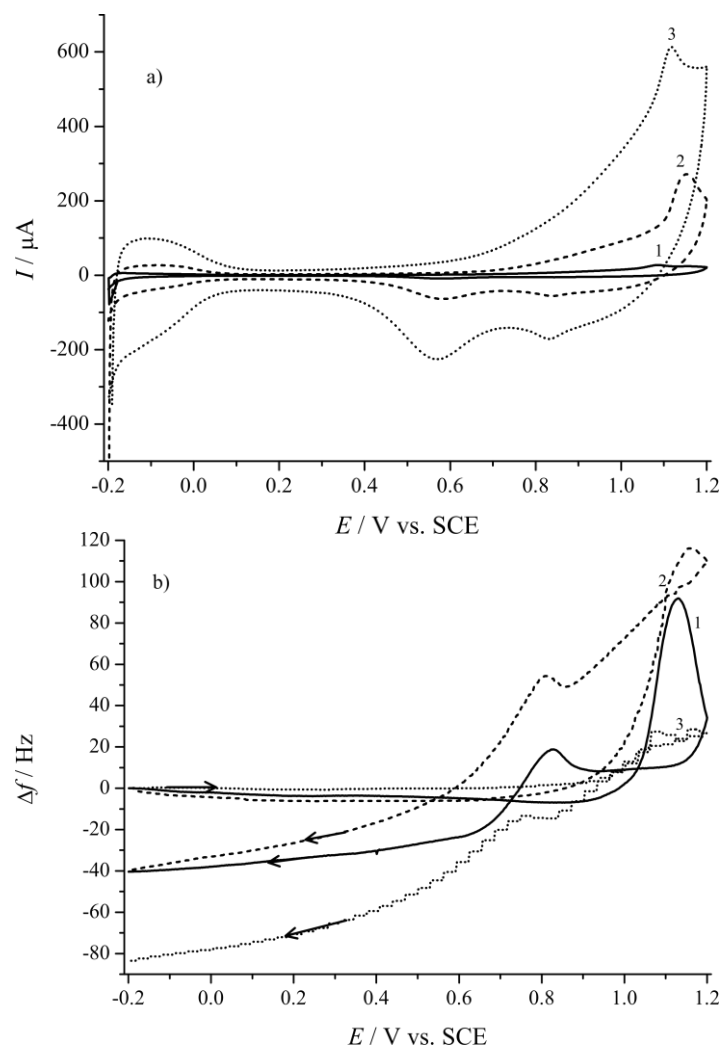


Fig. 8. a) Cyclic voltammograms and b) EQCN curves for PdPc microcrystals deposited on Pt. Electrolyte: 1 mol dm⁻³ deaerated sulfuric acid. Scan rates: 1) 5, 2) 20 and 3) 100 mV s⁻¹.

It could be concluded that the substrate–phthalocyanine interaction only slightly affected the voltammetric response at least compared to the behaviors of the layers on PIGE, Au and Pt, respectively. Under the same conditions (electrolyte composition, scan rate, potential region), the shift of the characteristic peak potentials was less than *ca.* 30 mV.

Effect of pH

On replacing sulfuric acid with a Na₂SO₄ solution, the respective waves appeared; however, as expected for any pH-dependent process, they were shifted

in the direction of more negative potentials (Fig. 11). This pH effect will be analyzed later because the Na_2SO_4 solution is an unbuffered system, *i.e.*, a pH change could occur near the electrode surface when protons are released or consumed. Experiments in the presence of phosphate buffers were also performed. However, a decreased electrochemical activity was observed when phosphate ions were present.

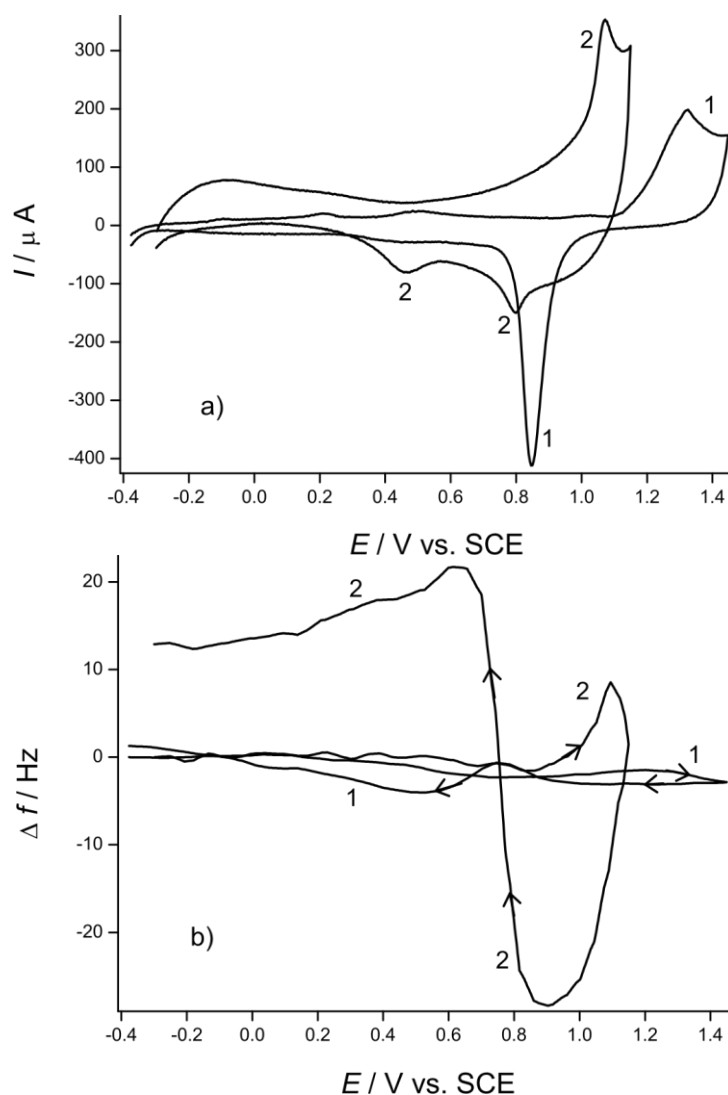


Fig. 9. a) Cyclic voltammograms and b) the simultaneously obtained EQCN frequency changes for 1) a gold electrode and 2) an Au|PdPc layer. Electrolyte: 0.5 mol dm^{-3} deaerated sulfuric acid. Scan rate: 100 mV s^{-1} .

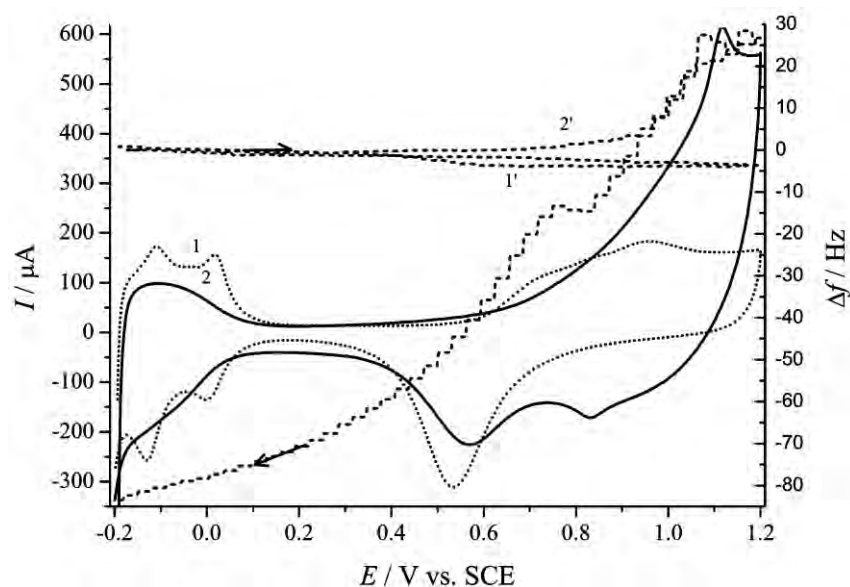


Fig. 10. Cyclic voltammograms (dotted line 1 Pt, continuous line 2 Pt|PdPc) and the simultaneously obtained EQCN frequency changes (dashed line 1' Pt, dashed line 2' Pt|PdPc) for 1) a platinum electrode and 2) a Pt|PdPc electrode. Electrolyte: 1 mol dm⁻³ deaerated sulfuric acid. Scan rate: 100 mV s⁻¹.

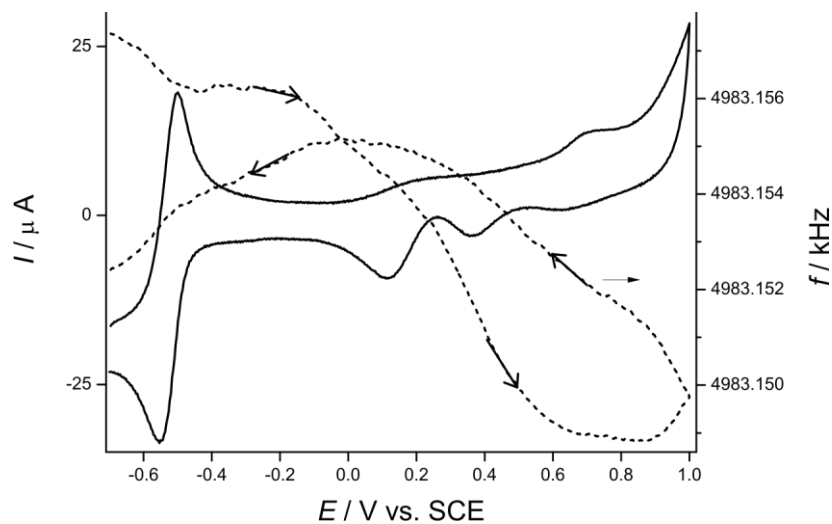


Fig. 11. Cyclic voltammogram (solid line) and the simultaneously obtained EQCN frequency curve (dashed line) obtained for PdPc microcrystals attached to Au. Electrolyte: 0.5 mol dm⁻³ deaerated Na₂SO₄ solution. Scan rate: 5 mV s⁻¹.

At *ca.* -0.5 V, a reversible pair of waves developed, which could be assigned to the hydrogen redox reaction since further reduction and re-oxidation of Pc ring

would involve a higher mass change due to the ionic exchange process. Nevertheless, it cannot be excluded that the redox reaction of PdPc contributes to this pair of waves, if protonation and deprotonation, respectively, occur. The EQCN curve is also of interest. Instead of the almost constant mass observed in acidic solutions, a frequency decrease (mass increase) was observed that commenced at wave II_a. In the region of wave I_a, the measured surface mass decreased again, as was also observed in acidic solution. Passing the reduction wave (II_c), the mass increased again. At the end of the cycle, the mass of the electrode was higher than its initial value. After several cycles at higher scan rates, the frequency returned to its starting value. This means that anions were incorporated and that a certain number of these ions remained permanently in the layer. Such an effect was previously observed *e.g.*, for PtPc layers in organic media.²¹ As the peak potentials depend on the pH, the deprotonation accompanying the redox processes still prevails and positive charges appear in the PdPc layer that are compensated by the negatively charged counter-ions. In neutral media, the participation of the cations, in this case Na⁺ cannot be excluded, either, since it was detected in the course of voltammetric studies of CoPc.¹⁸

In NaOH solution, all the waves appeared although the anodic waves were rather stretched while the cathodic peaks were well developed (Fig. 12). The EQCN response was substantially different from those measured in acidic or neutral solutions. At high negative potentials, a rather large, reversible frequency change was observed. During the anodic scan, this frequency increase was followed by a frequency decrease in the potential region of wave II_a. Reaching

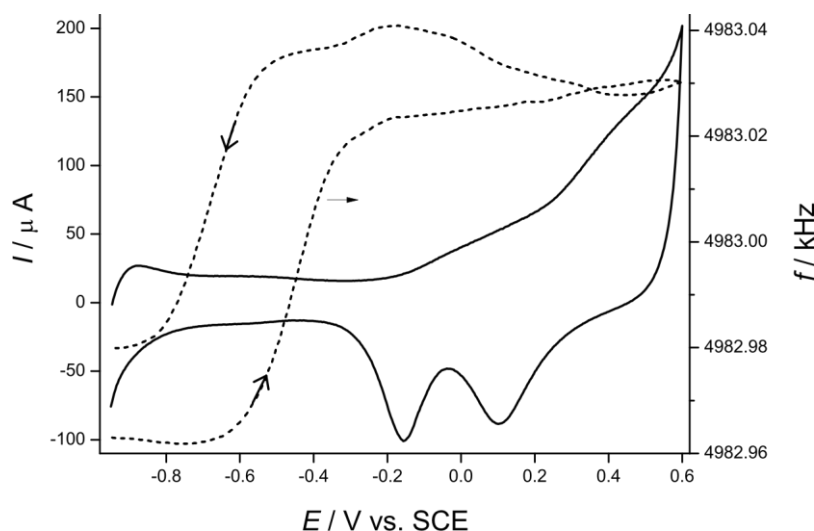


Fig. 12. Cyclic voltammogram (solid line) and the simultaneously obtained EQCN frequency curve (dashed line) obtained for PdPc microcrystals attached to Au. Electrolyte: 0.1 mol dm⁻³ NaOH + 0.4 mol dm⁻³ deaerated Na₂SO₄ solution. Scan rate: 50 mV s⁻¹.

the region of wave I_a , a small frequency increase again occurred. After potential reversal, slight mass increases occurred in two steps at the two cathodic waves, and eventually below *ca.* -0.4 V, the mass increased steeply until *ca.* -0.7 V. The apparent molar mass that could be calculated in this potential region was $M = 1025 \pm 75$ g mol $^{-1}$ for both the oxidation and the reduction processes.

A comparison of the pH dependence of the voltammetric and EQCN responses can be found in Fig. 13.

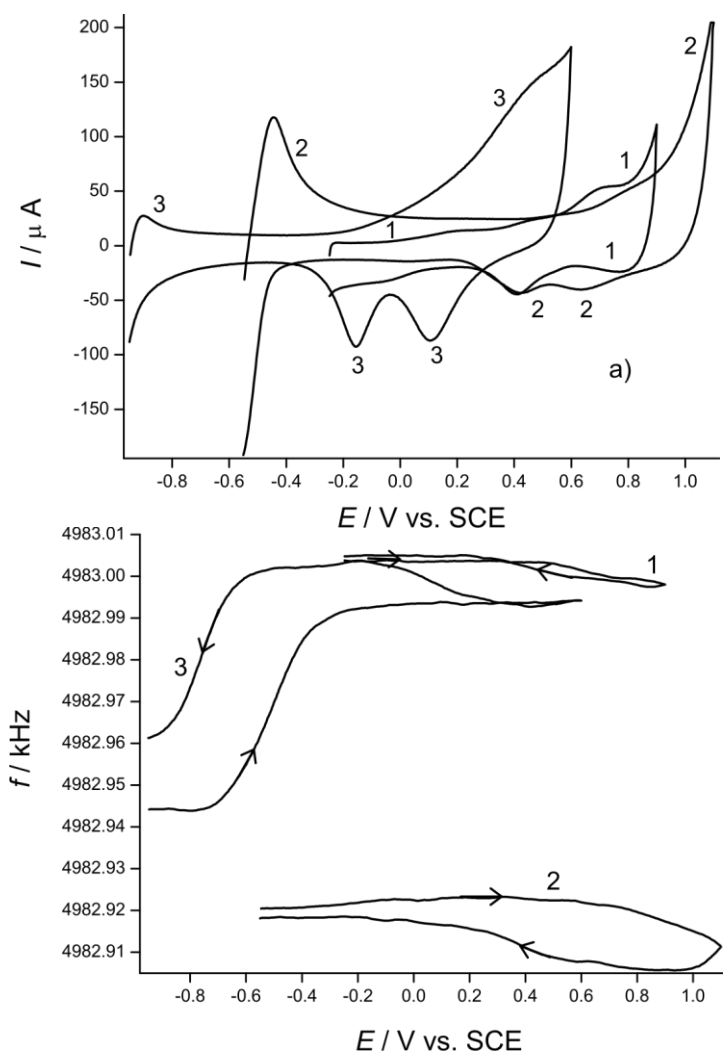
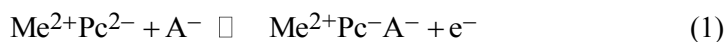


Fig. 13. a) Cyclic voltammograms and b) the simultaneously obtained EQCN frequency curve obtained for PdPc microcrystals attached to Au. Electrolyte: 1) 0.5 mol dm $^{-3}$ sulfuric acid, 2) 0.5 mol dm $^{-3}$ Na $_2$ SO $_4$ and 3) 0.1 mol dm $^{-3}$ NaOH + 0.4 mol dm $^{-3}$ deaerated Na $_2$ SO $_4$ solution. All solutions were deaerated with argon. Scan rate: 50 mV s $^{-1}$.

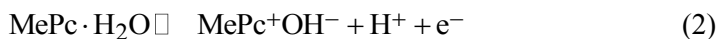
It is difficult to compare the peak potentials for the anodic peak. However, the potential shifts in the cases of waves I_c and II_c were found to be 700 and 600 mV, respectively, which was similar to the value of -780 mV expected for a H⁺/e⁻ process. Therefore, H⁺ ions certainly participate in the electrochemical transformations of PdPc. The changes of shape and magnitude of the EQCN responses show an increasing participation of species heavier than protons, which are obviously anions.

Usually, a rather simple scheme for the electrochemical transformations has been suggested when the central ion (*e.g.*, Me = Mg, Pt or Pd) does not undergo a redox process:



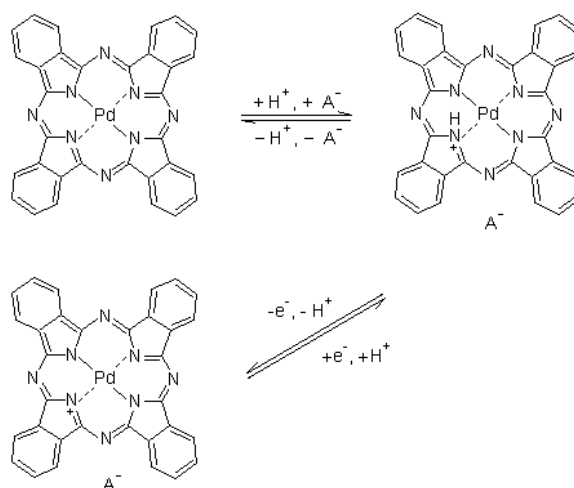
which, in the case of solid phase electrochemistry, necessarily involves the incorporation of an anion (A⁻) in the layer. The removal of an electron from the ring renders the phthalocyanine conductive.

However, it was also suggested¹⁰ that water molecules and/or OH⁻ could participate in the redox process as follows:



which may explain the observed pH dependence.

From the obtained EQCN results taking into account also the shift of the peak potentials, it can be assumed that PdPc is protonated in its reduced form in aqueous acidic media and counter-ions compensate the positive charge, which are already present in the surface layer of microcrystals. During oxidation, H₃O⁺ leaves the layer, and the exchange of anions is a minor process (see Scheme 1).



Scheme 1. The protonation equilibrium and the ionic exchange process during the electrochemical transformation of PdPc.

Surprisingly, the shift of the peak potentials as a function of concentration of sulfuric acid was previously assigned to the concentration changes of the anions,³³ albeit the shift observed was just the opposite to that expected based on the Nernst Law. However, an influx of protons was also assumed at short time scales. In sodium sulfate solutions, sorption and desorption of cations were also considered. With increasing pH and high positive potentials, the incorporation and expulsion of anions during the oxidation and reduction processes, respectively, would become the dominant process. In different non-aqueous solutions, only anion exchange was observed for conditioned PdPc layers,²⁹ which is understandable since no protonation could occur.

Of course, this is a rather simplified scheme since PdPc, as other metallic phthalocyanines, exists in different forms (monomeric and dimeric²⁹), it has different degrees of crystallinity that change during electrochemical treatments.³⁰ Phase transitions can also occur during electrochemical transformation, which manifest themselves in a large separation of the respective pairs of waves, since additional energy is required to create a solid–solid interface between the reduced and non-reduced forms.^{51–53} The phase transitions also influence the EQCN response because surface structural changes cause strain in the surface layer that can lead to anomalously large frequency changes (M values),^{53–58} *i.e.*, the M values that are calculated from the frequency change and the charge will not be the same as the molar masses of the exchanged, charged species, counter-ions or hydrated protons that enter the layer consisting of microcrystals to maintain electroneutrality. Solvent sorption–desorption accompanying the charging–discharging processes and the phase transition may also affect the M values that can be derived from the EQCN data. Phase transition and dehydration–hydration are the only explanation for the very high but reversible frequency change observed in alkaline media during the initial oxidation and re-reduction (Curve 3, Fig. 10), where $M = 1025 \pm 75 \text{ g mol}^{-1}$ was calculated. Other factors that should be considered for the elucidation of the rather complex mass change pattern as a function of potential are the spontaneous binding and removal of O_2 (especially when an oxygen-saturated solution is used), H_2O_2 (formed during the reduction of oxygen molecules) and OH^- in alkaline media, the effects of which depend on the nature of the central metal ion and are therefore responsible for the different catalytic activities.⁴¹

Detailed analysis of the EQCN responses

In order to emphasize the important features, two characteristic cyclic EQCN curves obtained after several cycles are discussed below.

When wave II_a appears, a mass decrease could be detected in this region in acidic solutions (Fig. 14). The calculated molar mass was $M = 20 \pm 2 \text{ g mol}^{-1}$, which may be interpreted as the loss of a H_3O^+ per electron. Although, some

detachment (dissolution) of the oxidized PdPc cannot be excluded, the observed effect is certainly due to the exchange of one or more species between the surface layer and the solution. (In the case of detachment, the mass loss would be permanent and higher, while here the original frequency value was more or less regained, albeit slowly.)

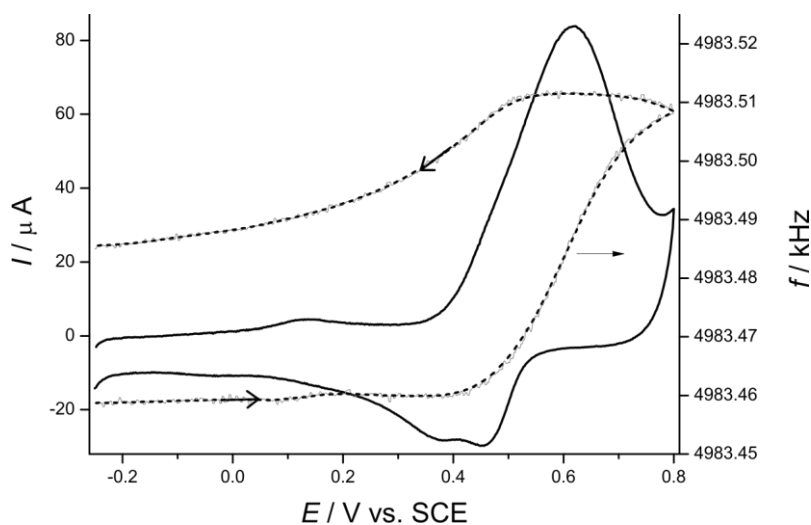


Fig. 14. Cyclic voltammogram (solid line) and the simultaneously obtained EQCN frequency curve (dashed line) obtained for PdPc microcrystals attached to Au. Electrolyte: 0.5 mol dm⁻³ deaerated sulfuric acid. Scan rate: 10 mV s⁻¹.

Even more instructive is the analysis of the EQCN curves obtained for a Pt-PdPc electrode at a slow scan rate (Fig. 15).

A slight mass increase could be observed in the region where no redox process occurs, *i.e.*, it is due to double layer charging. On reaching the region of peak I_a, a substantial frequency increase occurred. However, it became evident that wave I_a, in fact, consisted of two waves. At the second peak at more positive potentials, a large frequency decrease occurred that continued until positive current flowed during the reverse scan. No frequency change was observed until the reduction commenced at wave I_c, where a frequency increase occurred. However, this relatively small frequency increase was followed by a more intense frequency decrease that continued after wave II_c, with a lower slope until the end of the cathodic cycle. It is evident that no dissolution processes occurred in the regions of intense frequency increase, since at the end of the cycle, an overall mass gain was obtained. From the Δf vs. Q plots, the following values for the apparent molar masses were calculated. In the region of peak I_a, $M = 230.6 \pm 20$ g mol⁻¹ was calculated for the “mass decrease” (the error is estimated herein since it was calculated from this, single measurement), while for the “mass increase” at

the wave at the more positive potential $M = 213 \pm 20 \text{ g mol}^{-1}$ was found. There are two possible explanations. First, at low scan rates, there is enough time for the solvent transport to be completed, and the deprotonation was accompanied by intense dehydration of the PdPc layer. This was followed by the incorporation of hydrated anions. However, it is likely that a phase transition also occurred in this region, which was partially responsible for the dehydration–hydration processes. This is supported by the analysis of the cathodic scan where, at peak I_c , a frequency increase–decrease pattern was observed that is characteristic of phase transition processes and the respective stress generated in the surface layer as well as of dehydration–hydration phenomena.^{54–58} Here $M = 156 \pm 20 \text{ g mol}^{-1}$ and $258 \pm 20 \text{ g mol}^{-1}$ were calculated for the regions of frequency increase and decrease, respectively. For the potential region less positive than the peak potential of Π_a , a value of $M = 18 \pm 2 \text{ g mol}^{-1}$ was obtained, which might be due to slow rehydration of the layer.

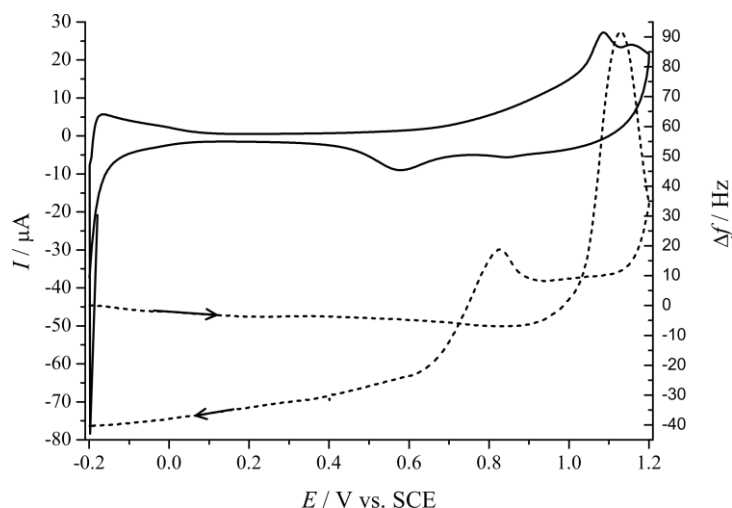


Fig. 15. Cyclic voltammograms (solid line) and the simultaneously obtained EQCN frequency changes (dashed line) for a Pt|PdPc electrode. Cycling was started from the open-circuit potential. Electrolyte: 1 mol dm^{-3} deaerated sulfuric acid. Scan rate: 2 mV s^{-1} .

CONCLUSIONS

The shape of the cyclic voltammograms, *i.e.*, the number of oxidation and reduction peaks and their relative ratios depend on several factors, such as the potential limits, presence and absence of oxygen, the type of the substrate, the nature and the concentration of the electrolyte, as well as the layer thickness and the method of the deposition.

In aqueous acidic media, PdPc is protonated in its reduced form and counterions compensate the positive charge; therefore, they are already present in the

surface layer. During oxidation, H_3O^+ leave the layer of microcrystals and the exchange of anions is a minor process in acid media except at high positive potentials. With increasing pH, the incorporation and expulsion of anions during the oxidation and reduction processes, respectively, becomes the dominant process.

Phase transitions also occur during the electrochemical transformations, which manifest themselves in the large separation of the respective pair of waves. The phase transition also influences the EQCN response because the surface structural changes cause strain in the surface layer, which leads to anomalously large frequency changes. Solvent sorption–desorption accompanies the charging–discharging processes and the phase transitions.

It was also observed that even at high positive potential limits, the presence of PdPc hinders the formation of gold or platinum oxide, respectively, as well as the hydrogen adsorption on Pt in the hydrogen UPD region.

Acknowledgements. Financial support of the National Scientific Research Fund (OTKA K100149) and TÁMOP-4.2.2/B-10/1-2010-0030 is gratefully acknowledged. One of the authors (Á. Nemes) is grateful for the support of the European Union and the State of Hungary, co-financed by the European Social Fund within the framework of TÁMOP 4.2.4. A/-11-1-2012-0001 “National Excellence Program”.

ИЗВОД

ЕЛЕКТРОХЕМИЈСКО И НАНОГРАВИМЕТРИЈСКО ИСПИТИВАЊЕ МИКРОКРИСТАЛА ПАЛАДИЈУМ-ФТАЛОЦИЈАНИНА

ÁKOS NEMES, COLIN E. MOORE и GYÖRGY INZELT

Department of Physical Chemistry, Institute of Chemistry, Eötvös Loránd University, Pázmány Péter sétány 1/A, 1117 Budapest, Hungary

Електрохемијска кварцна нановага је коришћена за испитивање редокс трансформација микрокристала паладијум-фталочијанина који су били депоновани на злато и платину у растворима различитих вредности рН. Да би се испитао ефекат супстрата, коришћена је и графитна електрода импрегнирана парафином. Показано је да су редокс трансформације паладијум-фталочијанина праћене процесима депротонације–протонације као и сорпције и десорпције јона супротног наелектрисања, респективно, при чему њихов степен зависи од вредности рН раствора. На основу резултата нанограмметријских мерења предложен је механизам који објашњава зависност поменутих процеса од рН. Такође је утврђено да се истовремено са процесима прелаза наелектрисања одигравају и фазни прелази чврсто–чврсто и транспорт воде.

(Примљено 9. септембра, ревидирано 19. септембра 2013)

REFERENCES

1. R. P. Linstead, *J. Chem. Soc.* (1934) 1016, 1017, 1022, 1027, 1031, 1033
2. A. B. P. Lever, J. P. Wilshire, *Can. J. Chem.* **54** (1976) 2514
3. J. Zagal, P. Bindra, E. Yeager, *J. Electrochem. Soc.* **78** (1978) 1345
4. B. Z. Nikolić, R. R. Adžić, E. B. Yeager, *J. Electroanal. Chem.* **103** (1979) 281
5. J. Zagal, P. Bindra, E. Yeager, *J. Electrochem. Soc.* **127** (1982) 1506

6. D. A. Scherson, S. B. Yao, E. B. Yeager, J. Eldridge, M. E. Kordesch, R. W. Hoffman, *J. Phys. Chem.* **87** (1983) 932
7. B. Simic-Glavaski, S. Zecevic, E. Yeager, *J. Electroanal. Chem.* **150** (1983) 469
8. G. C. S. Collins, D. J. Schiffrin, *J. Electrochem. Soc.* **132** (1983) 1835
9. O. Contamin, E. Levart, G. Mangner, R. Parsons, M. Savy, *J. Electroanal. Chem.* **179** (1984) 41
10. J. L. Kahl, L. R. Faulkner, K. Dwarakanath, H. Tachikawa, *J. Am. Chem. Soc.* **108** (1986) 5434
11. A. Elzing, A. Van der Putten, W. Visscher, E. Barendrecht, *J. Electroanal. Chem.* **233** (1987) 99
12. F. Castaneda, V. Plichon, *J. Electroanal. Chem.* **233** (1987) 77
13. F. Castaneda, V. Plichon, *J. Electroanal. Chem.* **236** (1987) 163
14. C. Paliteiro, A. Hamnett, J. B. Goodenough, *J. Electroanal. Chem.* **239** (1988) 273
15. P. He, J. Lu, C. Cha, *J. Electroanal. Chem.* **290** (1990) 203
16. P. He, P. Crouigneau, B. Beden, C. Lamy, *J. Electroanal. Chem.* **290** (1990) 215
17. R. Jansen, F. Beck, *Electrochim. Acta* **39** (1994) 921
18. S. Komorsky-Lovric, *J. Electroanal. Chem.* **397** (1995) 211
19. I. L. Kogan, K. Yakushi, *Electrochim. Acta* **43** (1998) 2053
20. J. Jiang, A. Kucernak, *J. Electroanal. Chem.* **490** (2000) 17
21. J. Jiang, A. Kucernak, *Electrochim. Acta* **45** (2000) 2227
22. J. Jiang, A. R. Kucernak, *Electrochim. Acta* **46** (2001) 3445
23. R. J. C. Brown, A. R. Kucernak, *Electrochim. Acta* **46** (2001) 2573
24. D. Geraldo, C. Linares, Y. Y. Chen, S. Ureta-Zanartu, J. H. Zagal, *Electrochem. Comm.* **4** (2002) 182
25. C. Linares, D. Geraldo, M. Paez, J. H. Zagal, *J. Solid State Electrochem.* **7** (2003) 626
26. C. A. Caro, J. H. Zagal, F. Bedioui, *J. Electrochem. Soc.* **150** (2003) E95
27. J. Mi, L. Guo, Y. Liu, W. Liu, G. You, S. Qian, *Phys. Lett., A* **310** (2003) 486
28. R. J. C. Brown, A. R. Kucernak, *J. Solid State Electrochem.* **9** (2005) 459
29. L. Gaffo, D. Goncalves, R. C. Faria, W. C. Moreira, O. N. Oliveira Jr., *J. Porphyrins Phthalocyanines* **9** (2005) 16
30. L. Gaffo, M. J. S. P. Brasil, F. Cerdeira, C. Giles, W. C. Moreira, *J. Porphyrins Phthalocyanines* **9** (2005) 89
31. P. A. Koca, H. A. Dincer, M. B. Kocak, A. Gül, *Russ. J. Electrochem.* **42** (2006) 31
32. M. Arıcı, D. Arıcan, A. Lütfi Ugur, A. Erdogmus, A. Koca, *Electrochim. Acta* **87** (2013) 554
33. R. J. C. Brown, D. J. L. Brett, A. R. J. Kucernak, *J. Electroanal. Chem.* **633** (2009) 339
34. K. Sakamoto, E. Ohno-Okumura, *Materials* **2** (2009) 1127
35. S. Yamazaki, N. Fujiwara, K. Yasuda, *Electrochim. Acta* **55** (2010) 753
36. Y. Yuan, B. Zhao, Y. Jeon, S. Zhong, S. Zhou, S. Kim, *Bioresour. Technol.* **102** (2011) 5849
37. I. A. Akinbulu, K. I. Ozoemena, T. Nyokong, *J. Solid State Electrochem.* **15** (2011) 2239
38. I. Ponce, J. F. Silva, R. Onate, M. C. Rezende, M. A. Páez, J. Pavez, J. H. Zagal, *Electrochem. Comm.* **13** (2011) 1182
39. C. Selvaraj, N. Munichandraiah, L. G. Scanlon, *J. Porphyrins Phthalocyanines* **16** (2012) 255
40. A. O. Ogunsipe, M. A. Idowu, T. B. Ogunbayo, I. A. Akinbulu, *J. Porphyrins Phthalocyanines* **16** (2012) 885
41. J. Guo, H. He, D. Chu, R. Chen, *Electrocatalysis* **3** (2012) 252

42. J. H. Zagal, I. Ponce, D. Baez, R. Venegas, J. Pavez, M. Paez, M. Gulppi, *Electrochem. Solid-State Lett.* **15** (2012) B90
43. *Phthalocyanines: Properties and Applications*, Vols. 1–4, C. C. Leznoff, A. P. B. Lever, Eds., VCH Publ., New York, 1989–1996,
44. G. de la Torre, M. Nicolau, T. Torre, in *Phthalocyanines: Properties and Applications and Electroactive Materials*, H. S. Nalwa, Ed., Academic Press, New York, 2001, pp. 1–111
45. N. M. Alpatova, E. V. Ovsyannikova, in *Electropolymerization*, S. Cosnier, A. Karyakin, Eds., Wiley–VCH, Weinheim, Germany, 2010, p. 111
46. F. Scholz, U. Schröder, R. Gulaboski, *Electrochemistry of Immobilized Particles and Droplets*, Springer, Berlin, 2005, p. 114
47. B. B. Berkes, A. Székely, G. Inzelt, *Electrochem. Commun.* **12** (2010) 1095
48. G. Inzelt, B. B. Berkes, Á. Kriston, *Electrochim. Acta* **55** (2010) 4742
49. G. Sauerbrey, *Z. Phys.* **155** (1959) 206
50. F. Scholz, B. Meyer, in *Electroanalytical Chemistry, A Series of Advances*, Vol. 20, A. J. Bard, I. Rubinstein, Eds., Marcel Dekker, New York, 1998, p. 1
51. R. Ramaray, C. Kabbe, F. Scholz F, *Electrochem. Commun.* **2** (2000) 190
52. F. Scholz, M. Lovric, Z. Stojek, *J. Solid State Electrochem.* **1** (1997) 134
53. M. F. Suárez, A. M. Bond, R. G. Compton, *J. Solid State Electrochem.* **4** (1999) 24
54. C. D. Evans, J. Q. Chambers, *Chem. Mater.* **6** (1994) 454
55. M. Hepel, W. Janusz, *Electrochim Acta* **45** (2000) 3785
56. J. Wang, L. M. Frostman, M. D. Ward, *J. Phys. Chem.* **96** (1992) 5224
57. G. Inzelt, Z. Puskas, *Electrochem. Commun.* **6** (2004) 805
58. G. Inzelt, A. Róka, *Israel J. Chem.* **48** (2008) 185.